

Channel prior based Retinex model for underwater image enhancement

Sathvik Srinivas

*Department of Electronics and
Communication Engineering
PES University
Bengaluru, India*

sathvik.srini@gmail.com

V. Ramakrishna Siddharth

*Department of Electronics and
Communication Engineering
PES University
Bengaluru, India*

vsiddharth2000@gmail.com

Surya Dutta

*Department of Electronics and
Communication Engineering
PES University
Bengaluru, India*

suryadutta240@gmail.com

Nikhil S. Khare

*Department of Electronics and
Communication Engineering
PES University
Bengaluru, India*

nikhilkhare51@gmail.com

Lavanya Krishna

*Department of Electronics and
Communication Engineering
PES University
Bengaluru, India*

lavanyakrishna@pes.edu

Abstract—Since light undergoes absorption and scattering when it travels in water, images taken under water fall prey to color distortion, fuzziness/haziness, underexposure, and color cast. To alleviate these issues, this paper proposes a novel Retinex-based enhancing approach aimed at enhancing low-quality underwater images. Firstly, the input image undergoes pre-processing, where a color correction technique is employed to address the problem of color distortion. This is followed by conversion of the input image from the Red, Green and Blue color space to the Lab color space. Then, by means of the multi scale Retinex, the illumination component of the image is procured. Image dehazing algorithms, i.e., bright channel prior and underwater dark channel prior algorithms are applied individually on the procured illumination component. The image gets enhanced and is then converted back to the Red, Green and Blue color space from the Lab color space. The final enhanced image is obtained by performing histogram equalization on the enhanced Red, Green and Blue image. This is intended to make the output color intensity more realistic. The efficacy of the algorithms are gauged by means of some image quality metrics. Compared to pre-existing techniques, the method proposed manages to effectively enhance images while keeping detail loss to a minimum.

Index Terms—Underwater Image Enhancement, Retinex model, Multi Scale Retinex, Lab color space, Underwater Dark Channel Prior, Bright Channel Prior

I. INTRODUCTION

Underwater images are of paramount importance in underwater scientific missions aimed at monitoring sea life and assessing the geological or biological environment. They are also used for the development and utilisation of deep-sea resources.

Now, a question that arises would be, “*What is the need to process these underwater images?*”.

To answer this, a closer examination of the Light absorption and scattering problem is needed. It is the chief reason for degradation of the quality of underwater images. It is known

to cause problems in captured images like color distortion, contrast reduction, fuzziness/haziness, underexposure and so on.

The Light Absorption and Scattering problem: The marine environment has suspended particles which absorb light and then re-emit it, thus scattering it. This process leads to attenuation of light as it goes deeper and deeper. It is important to note that different wavelengths of light get absorbed by the medium differently. The red color is absorbed first owing to its high wavelength whereas the green and blue colors are not absorbed as much. Consequently, the green and/or blue color predominate and the same is observed in all images captured under water. This is called color cast and is a recurrent type of color distortion.

The particles in the marine environment also reflect light back to the camera which interferes with the object’s reflected light. This is a key reason for the fuzziness and the poor contrast observed in underwater images. Many distant images are blurred in consequence. Furthermore, attenuation of underwater brightness is known to cause underexposure which is another issue having an adverse impact on the quality of underwater images.

Artificial light can be used to illuminate the scene. However, it is susceptible to light absorption and scattering as well, and hence, does not result in uniform lighting. Backscattering of light is another ill-effect of this, which leads to bright spots at the centre of the images and poor lighting at the periphery, which is not a desirable effect.

Thus, to overcome the aforementioned limitations, underwater image enhancement methods including underwater image dehazing algorithms, contrast enhancement algorithms are devised to improve specific image characteristics like color, contrast and brightness.

This paper explores the Retinex model and the impact that incorporation of the bright channel prior and underwater dark channel prior algorithms has on the quality of an underwater image.

II. SURVEY OF LITERATURE

A. The Retinex model

Retinex – “Retina” + “Cortex”

Land and McCann [1] exemplified the unusual nature of the human visual system and enunciated that the more widely-used color vision theory cannot explain it. They postulated the Retinex theory which states that the human visual system is an efficient information stabilizer that can extract constant information from a scene irrespective of the lighting conditions. This is called the color constancy mechanism of the human visual system. Since then, the Retinex theory has been used to drive various algorithms which aim to better the contrast of images with large dynamic range. As Retinex aligns with the human visual system, it is considered as a human-perception based image enhancement mechanism based on the method of illumination compensation. Retinex based algorithms provides color constancy as well as dynamic range compression.

These color constancy based techniques alter the RGB intensity values at each pixel and provide a good estimate of the color information present in an image, without requiring prior information about illumination. As a result, these Retinex-based algorithms improve the visual rendition of images when lighting conditions are bad. To sum up, Retinex attempts to balance machine and human vision, and ensure color constancy at the same time.

An image scene in a human being’s eyes can be modelled as the product of its illumination and reflectance. Let $I(x, y)$ represent the intensity of a pixel in the image I . Then,

$$I(x, y) = R(x, y) \times L(x, y)$$

where R is the reflectance and I is the illumination. Tang, Dong, Ma, Zhou and Li [2] make use of this model of the image to explain the Retinex model. The basic idea here is to employ various ways to extract the illumination component. Reflectance is obtained by the subtraction of the illumination from the original image. Finally, after appropriate enhancement, combination of the transformed illumination and reflectance components gives the final enhanced image. As a result, the naturalness of the enhanced images is preserved whereas other details can be enhanced. Retinex algorithms can be categorized into centre/surround based, recursive and path-based algorithms.

1) *The Single Scale Retinex:* The single scale Retinex is a centre/surround based Retinex algorithm. As previously introduced, the Retinex model regards an image I as the product of $R(x, y)$ and $L(x, y)$. For each pixel (x, y) , $L(x, y)$ represents its illumination and $L \in [0, 255]$ whereas $R(x, y)$ represents its reflectance and $R \in [0, 1]$. Note that I varies from 0 to 255. Lenka and Khandual [3] explain that $L(x, y)$ is based on the characteristic nature of the illumination source, whereas $R(x, y)$ can be found from the imaged objects’ characteristics.

The following constraints/assumptions are also to be made when evaluating an image using this model –

- 1) The illumination of the image should be spatially smooth.
- 2) R varies from 0 to 1, which implies that L is always greater than or equal to I .
- 3) The reflectance is a high frequency component, i.e., texture and edge related information. On the other hand, the illumination component is a low frequency component.

Since the illumination is a low frequency component, a low-pass filter can be employed to extract it. SSR is a centre/surround based Retinex technique. It makes use of a logarithmic photoreceptor function in order to approximate/emulate the human visual system. Reflectance is obtained through the single scale Retinex using the following:

$$R(x, y) = \log I(x, y) - \log[F(x, y) * I(x, y)] \quad (1)$$

where F represents the surround space function. It is a function that calculates the average of neighbouring pixel values and allocates it to the pixel at the centre. The choice of surround space function influences the amount of dynamic range compression produced. Using surround functions like the Gaussian and the exponential, result in good dynamic range compression. The Gaussian surround space function/Gaussian blur function is used here, which goes as follows:

$$F(x, y) = \frac{1}{2\pi\sigma^2} e^{-\frac{x^2+y^2}{2\sigma^2}}$$

Some of the features of SSR are highlighted by Lenka and Khandual [3] and are as follows:

- 1) As depicted by eq. 1, log transformation/placement is performed subsequent to incorporation of the surround function.
- 2) Violation of the grey world assumptions leads to greying out of images, either locally or globally or in rare cases, color distortion of images.

Rahman, Jobson and Woodell [4] exhibit the existence of a trade-off between the extent of dynamic range compression and the color/tonal rendition, which is to say, SSR is not capable of concomitantly imparting appreciable dynamic range compression as well as decent color rendition. Due to this trade-off, only one factor can be improved, which is done at the cost of the other. Adding to this, some detail loss also occurs because the surround space function (Gaussian filter) which is used causes image blurring. To remedy these problems, the multi scale Retinex was postulated.

2) *The Multi Scale Retinex:* In the hope of preserving both dynamic range compression and color rendition of an image, the multi scale Retinex (MSR) was introduced. The multi scale Retinex is represented as a weighted summation of a certain number of scales of the single scale Retinex [3]. It is also computationally fast because the different samples are processed in a parallel manner. This technique is aimed at achieving gamma correction, dynamic range compression, color constancy processing and color enhancement.

MSR is mathematically defined as shown:

$$R_{MSR} = \sum_{n=1}^N \omega_n R_n$$

or

$$R_{MSR} = \sum_{n=1}^N \omega_n \{ \log I(x, y) - \log [F_n(x, y) * I(x, y)] \}$$

where R_n represents the reflectance component associated with the n^{th} scale, ω_n represents the weight of the n^{th} scale and N is the chosen number of scales. F is the Gaussian surround space function, and it holds the same definition as used in the single-scale Retinex, i.e.,

$$F(x, y) = \frac{1}{2\pi\sigma^2} e^{-\frac{x^2+y^2}{2\sigma^2}}$$

Therefore, the essence of the multi scale Retinex lies in the weights used and the number of scales needed [3], [4].

The multi scale Retinex combines several weightings of the single scale Retinex, selects the right number of scales and also finds scales which can potentially be merged. It has been observed that three scales suffice for most images. Next, the best weights are chosen such that maximum dynamic range compression as well as color/tonal rendition can be obtained. However, the weights can be fine-tuned to incline more towards dynamic range compression or towards color/tonal rendition or maintain a balance between the two. Usually, equal weights gives creditable results. Therefore, parameters can be tailored to requirements which is what makes this technique attractive.

Images enhanced through MSR have substantial amount of dynamic range compression at the edges separating dark and light parts and decent color/tonal rendition in the entire image scale. Thus, MSR accounts for illumination differences in order to emulate what humans perceive in a scene.

The surround space function in MSR is the same as that of SSR, i.e., the Gaussian surround function. Also, logarithmic transformation is applied after the surround space function evaluation, similar to what has been done in the case of SSR.

MSR is observed to preserve most of the detail in the scene. Therefore, the multi scale Retinex produces a much better final enhanced image when considering color and dynamic range compression, when compared to the single scale Retinex.

However, even in the multi scale Retinex, it is hard to judge the fidelity of the reproduction of color. Consequently, there may be some issues pertaining to color sensitivity. Also, images enhanced by means of MSR still suffer from greying-out of uniform zones and hence, the overall result of enhancement through MSR is still more saturated than human observation. This gives the final image a washed-out appearance. These are some of the wrinkles in the multi scale Retinex that need to be ironed out.

As a whole, the multi scale Retinex is a very propitious method for underwater image enhancement. Research is always being conducted to incorporate other transmission-map

based, histogram-based and variational-optimization based approaches in conjunction with Retinex models to get better enhancement of images. The aim here is to incorporate transmission-map based approaches (prior-based algorithms) in a Retinex model.

B. The General Dark Channel Prior Algorithm

The General Dark Channel Prior algorithm is an image dehazing algorithm taking a hazy image input I . Marques, Albu and Hoeberichts [5] mathematically modelled this image as shown:

$$\begin{aligned} I(x) &= J(x)t(x) + A(1 - t(x)) \\ t(x) &= e^{-\beta d(x)} \end{aligned} \quad (2)$$

Here, I is the observed intensity (i.e., the input hazy image) whereas the dehazed image is represented by J (scene radiance). t is the transmission map which depicts the light reaching the camera without getting scattered or absorbed, A represents atmospheric light, β is the scattering coefficient of the atmosphere and d is the scene depth.

The objective here is to find J by quantitatively determining A and t for the given input image I . There are four steps involved in this process:

- 1) *Finding the dark channel:* The dehazing process starts with the calculation of the dark channel. Ω is a square patch centred at pixel x and having a fixed size. For such a patch, the dark channel is an image, composed of the pixel with the lowest intensity in that patch, factoring in all the channels. Marques, Albu and Hoeberichts [5] present the dark channel prior (DCP) as hinged on the assumption that the intensity of at least one pixel in one of the three color channels of underwater images will be very less, i.e., J^{dark} will tend to 0. This is supported by He, Sun and Tang [6] who proved that a large majority of pixels in the dark channel have zero intensity, thus backing the dark channel prior assumption. Therefore,

$$J^{dark}(x) = \min_{y \in \Omega(x)} (\min_{c \in \{r, g, b\}} J^c(y)) \rightarrow 0 \quad (3)$$

- 2) *Finding atmospheric light A:* A is deemed as the most haze-opaque region in the image. It can be determined by first choosing the 0.1% brightest pixels in the dark channel.

The next step can be carried out in two ways, either by evaluating the mean of these 0.1% brightest pixels, or by directly considering the intensities of the red, blue and green channels associated with the brightest pixel, as the atmospheric light A .

After finding A , eq. 2 is normalized with A . This is done independently for each channel $c \in \{r, g, b\}$ as shown:

$$\frac{I^c(x)}{A^c} = t(x) \frac{J^c(x)}{A^c} + 1 - t(x) \quad (4)$$

- 3) *Finding the transmission map t(x):* To obtain transmission map, consider the normalized hazy image equation 4. The minimization operator is applied and J is then substituted with 0 in accordance with the principle of

dark channel prior. The algorithm assumes the transmission in a patch as constant and hence t is independent of the minimization operator as shown below:

$$\min_{y \in \Omega(x)} \left(\min_c \frac{I^c(y)}{A^c} \right) = t(x) \min_{y \in \Omega(x)} \left(\min_c \frac{J^c(y)}{A^c} \right) + 1 - t(x) \quad (5)$$

Here, A^c is the atmospheric light in each color channel and its value ranges from 0 to 1. Also, the coefficient of $t(x)$ is equal to 0 (from eq. 3, $\min_{y \in \Omega(x)} (\min_{c \in \{r,g,b\}} J^c(y)) \rightarrow 0$ and A^c is always positive). Substituting and rearranging the terms, the expression for the transmission map $t(x)$ turns out to be

$$t(x) = 1 - \omega \min_{y \in \Omega(x)} \left(\min_c \frac{I^c(y)}{A^c} \right)$$

where $\omega \in (0, 1)$ and $A^c \in [0, 1]$

Now, it is common knowledge that haze happens to be a fundamental problem in images having faraway objects. This haze is attributed to the suspended particles in the medium. This should be removed so as to get relatively clearer images. However, there is one problem. It involves a phenomenon called aerial perspective which expounds that the haze present in images is instrumental in depth perception. Complete removal of haze may cause the image to seem unrealistic along with a loss of depth perception.

Therefore, a variable amount of haze is retained for the sake of perceiving faraway objects [6]. This is done by including a constant parameter ω ($0 < \omega < 1$). The value of ω is based on respective use-cases and more haze can be preserved adaptively for more faraway objects. By doing so, more realistic images can be expected after the dehazing process.

- 4) *Recovery of Scene Radiance:* The last step is to recover the scene radiance which is essentially the haze-less image. It involves using the obtained transmission map and atmospheric light to get J as shown in this equation. The recovered scene radiance is susceptible to noise where the denominator in the expression comes close to zero. Therefore, a lower bound t_0 to the transmission map $t(x)$ is defined, i.e., a small amount of haze is preserved in very haze-dense regions. This is akin to what is being done by the parameter ω .

The expression for scene radiance $J(x)$ (obtained from rearranging eq. 2) is as follows:

$$J(x) = \frac{I(x) - A}{\max(t(x), t_0)} + A$$

Upon recovery of scene radiance, a shortcoming is observed in the recovered image, which is the presence of blocking artifacts and halos. This is because the assumption that the transmission is always constant in a patch is not always true. Therefore, this is a downside of this algorithm.

C. Underwater Dark Channel Prior Algorithm

The Underwater Dark Channel Prior algorithm is modelled as a special case of the general dark channel prior algorithm but yields better results for underwater images when compared to the general algorithm. The difference lies in the fact that for the underwater dark channel prior, only the green and blue channels are considered during computation. On the other hand, as stated before, all three channels are involved in the general algorithm.

Now comes the main question: “*Why is the reason behind incorporating this? Isn’t the general algorithm good enough?*” Drews-Jr, do Nascimento, Moraes, Botelho and Campos [7] quote two reasons for this. Firstly, it is difficult to model red channel behaviour when it comes to underwater images. As mentioned in the introduction, with depth, the medium absorbs different wavelengths differently. Red is absorbed the most, resulting in a dominance of the green and/or blue color (color cast) in the underwater imagery. As a result, many pixels in the red channel have an intensity close to zero which makes the channel difficult to handle. This is largely observed in images having shadows, or underwater objects like fishes, algae, corals or rocks.

The second reason for omission of the red channel is a consequence of the first stated reason. It has been seen experimentally that the transmission estimate gets corrupted because of the many pixels being dark in the red channel. This causes the general dark channel prior algorithm to fail when restoring most underwater images.

Quantitative treatment of the algorithm: The image is modelled in the same way as in the general dark channel prior algorithm, i.e.,

$$I(x) = J(x)t(x) + A(1 - t(x))$$

However, the expression of $J^{dark}(x)$ in the case of UDCP takes into consideration only the green and blue channels [7] as shown:

$$J^{dark}(x) = \min_{y \in \Omega(x)} \left(\min_{c \in \{g,b\}} J^c(y) \right) \rightarrow 0$$

To find the atmospheric light A , the intensity of the brightest pixel in each of the two channels is chosen as the atmospheric light. Next, the transmission map is obtained by substituting the value of J ($= 0$) in the normalized image equation, like in the case of the general dark channel prior algorithm. The expression for scene radiance also remains the same but with c only composed of the green and blue channel. Also similar to the general algorithm is the presence of the parameters ω and t_0 which intend to preserve some haze so as to obtain realistic images.

$$t(x) = 1 - \omega \min_{y \in \Omega(x)} \left(\min_c \frac{I^c(y)}{A^c} \right)$$

where $\omega \in (0, 1)$ and $A^c \in [0, 1]$

$$J(x) = \frac{I(x) - A}{\max(t(x), t_0)} + A$$

D. The Bright Channel Prior Algorithm

Sun and Guo [8] used the same model as the one employed for the dark channel prior to characterize the hazy image as shown:

$$\begin{aligned} I(x) &= J(x)t(x) + A(1 - t(x)) \\ t(x) &= e^{-\beta d(x)} \end{aligned} \quad (6)$$

The variables shown have the same meaning as the ones mentioned before. Following are the steps stipulated by the algorithm to find J :

- 1) *Finding the bright channel:* For a square patch Ω of a given size in the hazy input image, the bright channel is an image, consisting of the pixel having the highest value of intensity in that patch. This is done considering all three color channels. Thus, the bright channel is represented as

$$J^{bright}(x) = \max_{y \in \Omega(x)} (\max_{c \in \{r, g, b\}} J^c(y)) \quad (7)$$

- 2) *Finding atmospheric light A:* This is calculated in a fashion similar to that of the dark channel prior but the main difference lies in the fact that either the pixel with the lowest intensity or the mean of a group of pixels with lowest intensities (instead of highest) is considered while finding A .

After calculating A , eq. 6 is normalized with A for all $c \in \{r, g, b\}$ as shown (calculations for each channel done independently):

$$\frac{I^c(x)}{A^c} = t(x) \frac{J^c(x)}{A^c} + 1 - t(x) \quad (8)$$

- 3) *Finding the transmission map t(x):* The maximization operator is applied on both sides of eq. 8. Akin to what is done in the dark channel prior algorithm, the transmission is assumed to be constant in a local patch $\Omega(x)$ and hence is independent of the maximization operator as shown:

$$\max_{y \in \Omega(x)} \left(\max_c \frac{I^c(y)}{A^c} \right) = t(x) \max_{y \in \Omega(x)} \left(\max_c \frac{J^c(y)}{A^c} \right) + 1 - t(x) \quad (9)$$

Upon rearrangement of eq. 9, the expression for transmission map $t(x)$ is obtained as follows:

$$t(x) = \frac{\max_{y \in \Omega(x)} (\max_c I^c(y)) - A^c}{\max_{y \in \Omega(x)} (\max_c J^c(y)) + M - A^c}$$

Here, M is an optional brightness parameter which is adjusted according to the requirement of applications.

- 4) *Recovery of Scene Radiance:* The scene radiance can be procured from the computed atmospheric light and transmission map as shown in the following equation:

$$J(x) = \frac{I(x) - A}{\max(t(x), t_0)} + A$$

t_0 , is a constant aimed at limiting the lowest value of the denominator. This is for preservation of some haze.

III. PROPOSED METHOD

The proposed method is based on the Retinex-based model of image enhancement. Land and McCann [1] were the ones who proposed the Retinex theory and demonstrated that the human visual system (HVS) can deal with illumination that changes both brightness and color adaptively. The Retinex methods enhance the input image by extracting the illumination component using low-pass filters and logarithmic transformation. However, a halo effect is observed near the edges. Fu et al [9] proposed a BCP at the illumination to reduce said halo effects. In the course of research, it was also found that the incorporation of UDCP at the same stage gives an output which is comparable or in some cases, even better than that of the BCP approach, depending on the image and its features.

The proposed method has been divided into 3 sections :

- 1) Pre-Processing Steps - Color Correction and Conversion from RGB to Lab color space
- 2) Incorporation of BCP/UDCP into the Retinex Algorithm
- 3) Post-Processing steps

A. Pre-Processing

1) *Color Correction:* Color correction is an essential process in many fields where the light and the colors of an image are altered altogether. To address the color cast, a color correction technique based on a histogram equalization is being used. In histogram equalization, the contrast of each channel is enhanced, hence making the bright parts, brighter and the dark parts, darker.

The image is first divided into channels, which are red, green and blue. For every channel, the number of occurrences of each element in a flattened array is found, with values spanning from 0 to 255. The number of occurrences of each element is stored at the corresponding index in an array. High and Low values are found from the above array. After this, new values are assigned to each level. If a level is lesser than the Low value (lv), it is equated to zero and if it is greater than the High value (hv), it is equated to 255. For levels that lie in between the Low and High values, they are equated to a normalized value (shown below).

This assignment of values is depicted in the below expression:

$$level = \begin{cases} 0 & \text{if } level < lv \\ \frac{(level-lv)}{(hv-lv)} \times 255 & \text{if } lv \leq level \leq hv \\ 255 & \text{if } level > hv \end{cases}$$

This is repeated for every channel and finally, to obtain the output image, all the three channels are merged.

2) *Conversion of the RGB image to Lab:* The CIE Lab color space is a three-dimensional space which covers the whole range of human color perception.

In order to convert Red, Green and Blue (RGB) values to the Lab values, the reference illuminant of the RGB color space and the RGB primary co-ordinates are stored in the form of a color lookup table (CLUT), which is contained in most imaging and machine vision libraries and these are used to

perform these conversions. While RGB operates on 3 channels, i.e., red, green and blue, Lab is a conversion of the same information to a brightness (luminosity) component L, and 2 color components (channels) a and b.

The reason to do the conversion to Lab color space is because, firstly, since one entire channel is dedicated to luminosity, it can be kept separate from the color channels so that you can adjust one component without affecting the other. Secondly, the L component closely matches with the human visual system's perception of lightness. Therefore, brightening an image or performing color correction on an image in the CIE Lab color space causes the result to often look more accurate to the human visual system, color wise. Thirdly, by using the CIE Lab color space, colors can be shifted, and pictures can be made more vibrant without changing the amount of saturation present in them. Also, to-and-fro translations between RGB and Lab is lossless and this is very advantageous as information is not lost. Thus, Lab color space relates better with human color perception.

B. Incorporation of BCP/UDCP into the Retinex Algorithm

The L layer, i.e., the Luminance layer of the obtained Lab image is taken and the Illumination and Reflectance components of the image are extracted from it, as shown in the flowchart. Illumination is piecewise smooth whereas the reflectance is piecewise constant and contains edges. In the Retinex model, the illumination component is found using low-pass Gaussian filters and the reflectance component is found by the subtraction of the illumination component from the original image. Howbeit, a halo effect at object edges may be observed which is undesirable. This is due to the illumination component of the image being continuous near object edges. To tackle this problem, two approaches are used:

- 1) *BCP approach*: As mentioned above, the Retinex model based approach still suffers from a small halo effect because the illumination component is continuous near edges. To apply discontinuity, the bright channel prior algorithm is applied on the illumination component, which suppresses this halo effect. A pixel-wise bright channel is used to do this. This approach gives the enhanced reflectance and illumination components of the image.
- 2) *UDCP approach*: The UDCP algorithm, as mentioned previously, is specifically designed for underwater images where the red channel is not considered in the computation. This algorithm (applied pixel-wise in this case) has been proven to produce better images. The procedure is same as that of the BCP approach.

C. Post-Processing Steps

After obtaining the enhanced illumination and reflectance components, they are combined to get the L layer, i.e., the luminance layer. This, in turn, is merged with the a and b layers to get back the image in the Lab color space. The image obtained is converted back to the RGB color space to give an enhanced underwater image. Upon examination, the intensity

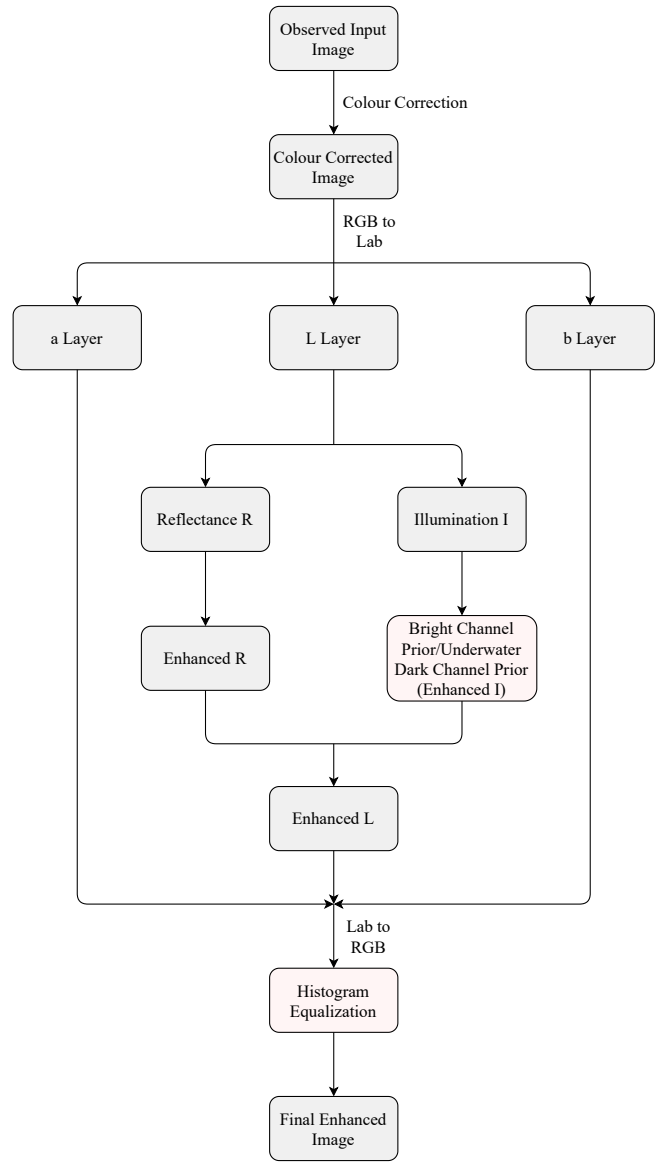


Fig. 1. Enhancement steps

of color in the resultant image was found to be high, leading to loss of realism. It was then realized that applying Histogram Equalization to that image normalizes the intensity of color in the image. The image obtained after applying Histogram Equalization is the final enhanced image.

IV. IMPLEMENTATION RESULTS

Conventionally, the reference images for the full-reference quality metrics (i.e., PSNR, UQI and SSIM) are clear and perfect images. A higher value implies better enhancement. However, contrary to the aforementioned notion, raw and fuzzy images were taken as reference images instead of clear images. Therefore, lower values denote higher quality output images and hence, a better enhancement technique.

The enhancement process was performed on a set of ten images. The results of three such images are shown in the next



(a) Image 1



(b) Image 2



(c) Image 3

Fig. 2. Fuzzy Images



(a)



(b)



(c)

Fig. 3. Images enhanced using MSR + BCP



(a)



(b)



(c)

Fig. 4. Images enhanced using MSR + UDCP



(a)



(b)



(c)

Fig. 5. Images enhanced using MSR + BCP + HE



(a)



(b)



(c)

Fig. 6. Images enhanced using MSR + UDCP + HE

TABLE I
METRIC VALUES OBTAINED FOR EACH ALGORITHM/TECHNIQUE

Technique	Image	<i>PSNR</i>	<i>UQI</i>	<i>SSIM</i>	<i>BRISQUE</i>
<i>ICM</i>	1	15.9663	0.891199	0.74878	28.9905
	2	18.6543	0.918214	0.77025	29.8363
	3	16.2096	0.862955	0.6076	34.0859
<i>UCM</i>	1	12.7136	0.76252	0.49101	27.8655
	2	14.7806	0.792083	0.52455	17.8036
	3	13.2104	0.717818	0.27536	28.5576
<i>Rayleigh distribution based enhancement</i>	1	9.197	0.566353	0.10108	30.8738
	2	10.9706	0.678524	0.092366	24.8483
	3	12.8327	0.749036	0.33985	17.255
<i>HE</i>	1	8.5424	0.529737	0.085879	31.4082
	2	10.5309	0.673682	0.065961	26.5064
	3	13.3239	0.804728	0.36099	14.5392
<i>SSR</i>	1	8.9718	0.499935	0.017244	31.9572
	2	10.5833	0.65653	0.099874	20.3398
	3	14.5341	0.86561	0.40065	18.942
<i>MSR</i>	1	8.5648	0.498147	0.091105	40.0024
	2	9.7926	0.624306	0.090361	38.8194
	3	13.8556	0.853623	0.30155	19.3171
<i>MSR + BCP</i>	1	9.1934	0.51809	0.12026	39.7587
	2	10.2407	0.637269	0.12305	38.77
	3	13.1804	0.802841	0.28263	18.2619
<i>MSR + UDCP</i>	1	9.5137	0.539194	0.13893	39.0188
	2	10.1705	0.621739	0.12982	38.0997
	3	12.9136	0.774712	0.27927	17.498
<i>MSR + BCP + HE</i>	1	8.0594	0.48443	0.03827	38.862
	2	8.9894	0.587129	0.035413	38.2744
	3	12.2732	0.782237	0.27027	23.1037
<i>MSR + UDCP + HE</i>	1	8.0371	0.485379	0.38297	38.0139
	2	8.7851	0.576418	0.03718	37.0443
	3	12.3088	0.782697	0.27204	22.2946

page. Table I depicts the values of metrics obtained for these three images. Along with the Retinex based techniques, metric values for other pre-existing techniques, namely, the Integrated color Model (ICM) [10], the Unsupervised color Correction Method (UCM) [11], Rayleigh distribution based enhancement [12] and Histogram Equalization (HE) [12] are depicted. This is done to compare the efficiency of the proposed methods with that of pre-existing methods.

A few observations on the metric results are given below:

- 1) *Peak Signal to Noise Ratio (PSNR)*: PSNR presents the combination of MSR, UDCP and HE as the best solution. The combination of MSR, BCP and HE also performs reasonably well. The difference in performance between the two is because of UDCP being a component of the former, which gives an edge over BCP in the case of underwater images.
- 2) *Universal Image Quality Index (UQI)*: According to the results obtained through UQI, the combination of MSR

and UDCP provide the best results. MSR + UDCP + HE and MSR + BCP + HE are not far behind in performance.

- 3) *Structural Similarity Index (SSIM)*: The SSIM metric is in agreement with the UQI metric with regard to the combination of MSR and UDCP being the best technique. Following closely behind is combination of MSR, BCP and HE. However, the metric results show that the MSR + UDCP + HE combination is not up to the mark. This implies that the results of this combination may not conform with the subjective score given by human perception of images.
- 4) *Blind/Referenceless Image Spatial Quality Evaluator (BRISQUE)*: According to BRISQUE, enhancement solely based on Rayleigh Distribution produces the best enhanced image. The proposed methods which are MSR + BCP + HE and MSR + UDCP + HE yield slightly high values of BRISQUE metric. Nevertheless, the results are

up to par.

Overall, it is evident that Retinex models involving UDCP generally perform better than ones with BCP (with the exception of SSIM). This is obvious because the UDCP algorithm is tailor-made for underwater images. Also, the proposed methods are relatively successful in keeping detail loss to a minimum, when compared to the other preexisting algorithms.

V. CONCLUSION

Owing to the light absorption and scattering problem, underwater images lose a considerable amount of detail. The aim was to find an effective technique to remedy this and prior to testing the proposed method, a host of pre-existing algorithms were surveyed. Then, the proposed methods, i.e., MSR + BCP and MSR + UDCP were implemented. The output color intensity was very high; ergo, Histogram Equalization was employed as a post-processing step to resolve this issue. Following implementation, four metrics were used to quantify the efficacy of each of the algorithms. The proposed techniques fared pretty well and the objective of minimizing detail loss was fulfilled.

VI. FUTURE WORK

As evident from the implementation results and conclusions, the problem of color cast and halo effect has been resolved. The loss of detail during this enhancement process is also minimum. However, when it comes to human perception of images, the SSIM metric, which aligns with human perception depicts the combination of MSR, BCP and HE as unsatisfactory. This would imply that images generated by this method are not up to par when perceived by humans. Newer techniques can be devised where images are pleasing to the human eye as well as not subject to detail loss.

Another problem encountered in the course of research involved images with predominant blue color. Enhancement of such images led to orange-red outputs which were highly unnatural.

REFERENCES

- [1] E. H. Land and J. J. McCann, "Lightness and retinex theory," *J. Opt. Soc. Am.*, vol. 61, no. 1, pp. 1–11, Jan 1971. [Online]. Available: <http://www.osapublishing.org/abstract.cfm?URI=josa-61-1-1>
- [2] S. Tang, M. Dong, J. Ma, Z. Zhou, and C. Li, "Color image enhancement based on retinex theory with guided filter," in *2017 29th Chinese Control And Decision Conference (CCDC)*, 2017, pp. 5676–5680.
- [3] R. Lenka and A. Khandual, "A study on retinex theory and illumination effects—i," *International Journal of Advanced Research in Computer Science and Software Engineering*, vol. 6, 01 2016.
- [4] Z. Rahman, D. Jobson, and G. Woodell, "Multi-scale retinex for color image enhancement," in *Proceedings of 3rd IEEE International Conference on Image Processing*, vol. 3, 1996, pp. 1003–1006 vol.3.
- [5] T. P. Marques, A. B. Albu, and M. Hoeberechts, "Enhancement of low-lighting underwater images using dark channel prior and fast guided filters," in *Pattern Recognition and Information Forensics*, Z. Zhang, D. Suter, Y. Tian, A. Branzan Albu, N. Sidère, and H. Jair Escalante, Eds. Cham: Springer International Publishing, 2019, pp. 55–65.
- [6] K. He, J. Sun, and X. Tang, "Single image haze removal using dark channel prior," *IEEE Transactions on Pattern Analysis and Machine Intelligence*, vol. 33, no. 12, pp. 2341–2353, 2011.
- [7] P. Drews Jr, E. do Nascimento, F. Moraes, S. Botelho, and M. Campos, "Transmission estimation in underwater single images," in *2013 IEEE International Conference on Computer Vision Workshops*, 2013, pp. 825–830.
- [8] S. Sun and X. Guo, "Image enhancement using bright channel prior," in *2016 International Conference on Industrial Informatics - Computing Technology, Intelligent Technology, Industrial Information Integration (ICIICTI)*, 2016, pp. 83–86.
- [9] X. Fu, Y. Sun, M. LiWang, Y. Huang, X.-P. Zhang, and X. Ding, "A novel retinex based approach for image enhancement with illumination adjustment," in *2014 IEEE International Conference on Acoustics, Speech and Signal Processing (ICASSP)*, 2014, pp. 1190–1194.
- [10] K. Iqbal, R. Abdul Salam, O. Azam, and A. Talib, "Underwater image enhancement using an integrated colour model," *IAENG International Journal of Computer Science*, vol. 34, 01 2007.
- [11] K. Iqbal, M. Odetayo, A. James, R. A. Salam, and A. Z. H. Talib, "Enhancing the low quality images using unsupervised colour correction method," in *2010 IEEE International Conference on Systems, Man and Cybernetics*, 2010, pp. 1703–1709.
- [12] A. S. A. Ghani and N. A. M. Isa, "Underwater image quality enhancement through composition of dual-intensity images and rayleigh-stretching," in *2014 IEEE Fourth International Conference on Consumer Electronics Berlin (ICCE-Berlin)*, 2014, pp. 219–220.
- [13] Y. Wang, W. Song, G. Fortino, L.-Z. Qi, W. Zhang, and A. Liotta, "An experimental-based review of image enhancement and image restoration methods for underwater imaging," *IEEE Access*, vol. 7, pp. 140233–140251, 2019.
- [14] J. Zhou, D. Zhang, and W. Zhang, "Multiscale fusion method for the enhancement of low-light underwater images," *Mathematical Problems in Engineering*, vol. 2020, pp. 1–15, 09 2020.
- [15] R. Schettini and S. Corchs, "Underwater image processing: State of the art of restoration and image enhancement methods," *EURASIP J. Adv. Signal Process*, vol. 2010, Jan. 2010. [Online]. Available: <https://doi.org/10.1155/2010/746052>
- [16] S. Park, B. Moon, S. Ko, S. Yu, and J. Paik, "Low-light image restoration using bright channel prior-based variational retinex model," *EURASIP Journal on Image and Video Processing*, vol. 2017, 06 2017.
- [17] X. Fu, P. Zhuang, Y. Huang, Y. Liao, X.-P. Zhang, and X. Ding, "A retinex-based enhancing approach for single underwater image," in *2014 IEEE International Conference on Image Processing (ICIP)*, 2014, pp. 4572–4576.
- [18] Y. Gao, H. Li, and S. Wen, "Restoration and enhancement of underwater images based on bright channel prior," *Mathematical Problems in Engineering*, vol. 2016, pp. 1–15, 11 2016.
- [19] E. Provenzi, L. D. Carli, A. Rizzi, and D. Marini, "Mathematical definition and analysis of the retinex algorithm," *J. Opt. Soc. Am. A*, vol. 22, no. 12, pp. 2613–2621, Dec 2005. [Online]. Available: <http://josaa.osa.org/abstract.cfm?URI=josaa-22-12-2613>
- [20] M. Tkalcic and J. Tasic, "Colour spaces: perceptual, historical and applicational background," in *The IEEE Region 8 EUROCON 2003. Computer as a Tool*, vol. 1, 2003, pp. 304–308 vol.1.
- [21] J. Chen and L.-P. Chau, "An enhanced window-variant dark channel prior for depth estimation using single foggy image," in *2013 IEEE International Conference on Image Processing*, 2013, pp. 3508–3512.
- [22] Z. Wang and A. Bovik, "A universal image quality index," *IEEE Signal Processing Letters*, vol. 9, no. 3, pp. 81–84, 2002.
- [23] W. Hao, M. He, H. Ge, C. jin Wang, and Q.-W. Gao, "Retinex-like method for image enhancement in poor visibility conditions," *Procedia Engineering*, vol. 15, pp. 2798–2803, 2011, cEIS 2011. [Online]. Available: <https://www.sciencedirect.com/science/article/pii/S1877705811020285>
- [24] Q.-N. Zhao, T.-Z. Huang, X.-L. Zhao, T.-H. Ma, and M.-H. Cheng, "A convex optimization model and algorithm for retinex," *Mathematical Problems in Engineering*, vol. 2017, pp. 1–14, 07 2017.
- [25] C. Li, C. Guo, W. Ren, R. Cong, J. Hou, S. Kwong, and D. Tao, "An underwater image enhancement benchmark dataset and beyond," *IEEE Transactions on Image Processing*, vol. 29, pp. 4376–4389, 2020.
- [26] A. A. Reddy, P. R. Jois, J. Deekshitha, S. Namratha, and R. Hegde, "Comparison of image enhancement techniques using retinex models," *International Journal of Advanced Computer Engineering and Communication Technology (IJACECT)*, vol. 2, 2013.
- [27] A. S. A. Ghani and N. A. M. Isa, "Underwater image quality enhancement through rayleigh-stretching and averaging image planes," *International Journal of Naval Architecture and Ocean Engineering*,

- vol. 6, no. 4, pp. 840–866, 2014. [Online]. Available: <https://www.sciencedirect.com/science/article/pii/S2092678216302588>
- [28] W. Song, Y. Wang, D. Huang, A. Liotta, and C. Perra, “Enhancement of underwater images with statistical model of background light and optimization of transmission map,” *IEEE Transactions on Broadcasting*, vol. 66, no. 1, pp. 153–169, 2020.
- [29] W. Song, Y. Wang, D. Huang, and D. Tjondronegoro, “A rapid scene depth estimation model based on underwater light attenuation prior for underwater image restoration,” in *Advances in Multimedia Information Processing – PCM 2018*, R. Hong, W.-H. Cheng, T. Yamasaki, M. Wang, and C.-W. Ngo, Eds. Cham: Springer International Publishing, 2018, pp. 678–688.
- [30] D. Huang, Y. Wang, W. Song, J. Sequeira, and S. Mavromatis, “Shallow-water image enhancement using relative global histogram stretching based on adaptive parameter acquisition,” in *MultiMedia Modeling*, K. Schoeffmann, T. H. Chalidabongse, C. W. Ngo, S. Aramvith, N. E. O’Connor, Y.-S. Ho, M. Gabbouj, and A. Elgammal, Eds. Cham: Springer International Publishing, 2018, pp. 453–465.
- [31] K. Barnard, V. Cardei, and B. Funt, “A comparison of computational color constancy algorithms. i: Methodology and experiments with synthesized data,” *IEEE Transactions on Image Processing*, vol. 11, no. 9, pp. 972–984, 2002.
- [32] R. C. Gonzalez and R. E. Woods, *Digital Image Processing*. Pearson, 2018, pp. 369–370. [Online]. Available: <https://books.google.co.in/books?id=0F05vgAACAAJ>